



The effect of shallow gas on the performance of pile foundation for offshore jacket platform in Malaysian Waters

N. N. Huang

PETRONAS, Kuala Lumpur, Malaysia

M. J. Rohani, A. A. Rahman, N. Yusoff, N. M. Fatimi, Z.A.M. Ali

PETRONAS, Kuala Lumpur, Malaysia

R. Ragni, S. Farhana, N. Boylan

Norwegian Geotechnical Institute (NGI), Perth, Australia

noorizal.nasrih@petronas.com

ABSTRACT: In 2023, gas bubbles were observed in the proximity of conductor and pile foundation of an offshore jacket platform, Platform BA. The objective of this study was to demonstrate the potential effect of shallow gas in soil to the pile axial and lateral response, and the offshore jacket platform performance. The presence of gas is linked to the development of excess pore pressure (XPP) in the soil. In turn, this affects the effective stresses in the soil and ultimately the soil response. First, axial capacity check was performed based on the soil response due to the presence of gas. Then, three different methods, namely, API, NGI-Petronas (NGI-P) and Jeanjean et al. (Jeanjean). The parameters from the Pile/Structure Interaction (PSI) assessments were then used in structural in-service condition analysis. Results from the axial capacity check indicates a reduction in axial capacity when considering the effect of XPP thus not meeting the required safety factors (SF). However, after considering ageing effects, Platform BA piles are still within code compliance. In terms of the lateral response, the NGI-P and Jeanjean methods simulate a stiffer response than API, leading to smaller lateral displacement at pile head. The magnitude of XPP in the gas-charged layer did not have a meaningful impact on the pile lateral response. This is attributed to the large depth of the gas-charged layer. In turn, the soil near seabed, which offers the largest lateral resistance, was mostly unaffected. Results from structural analyses indicate that the different P-Y approaches have minimal influence on the pile unity check for piles above and below mudline, up to 9% improvement on offshore jacket platform natural period and up to 7% improvement on offshore platform reserve strength ratio when adopting Jeanjean method.

Keywords: Shallow Gas; Excess pore pressure; Axial capacity Lateral response; Reserved strength ratio

1 BACKGROUND

Shallow gas can influence the bearing capacity of a pile significantly. Additionally, gas seepage may form craters, and if these craters appear around the top of a pile, they could affect the pile's lateral resistance (Lunne et al., 1996). BA field area is a known gas-prone field in Offshore Malaysia. In 2023, gas bubbles were observed close to location of pile foundation of an offshore jacket platform, Platform BA.

Site survey covering BA field area was done back in 2019, complement with P-Cable 3D seismic data. Results from the site survey indicates three seismic amplitude anomalies are present within a 1-kilometer radius of Platform BA. No recent soil investigation data was collected. Hence, the assessment on the soil data was done using a legacy soil data collected back in 1980. The objective of this study was to demonstrate the potential effect of gas in the soil on the pile lateral response and pile axial

capacity. The presence of gas is linked to the development of excess pore pressure (XPP) in the soil. In turn, this affects the effective stresses in the soil and ultimately the soil response laterally and axially.

The study involved the generation of (i) lateral response springs, also known as p-y curves, at regular intervals along the pile length to simulate the soil-pile interaction and (ii) axial capacity curves.

2 PLATFORM DETAILS

Platform BA is a 4-well cluster drilling platform, installed in July 1981 in the BA field in a water depth of 41.2m. The platform is founded on four main piles and three skirt piles, all of which are 24-inch OD. See Table 1 for details on pile geometry.

Table 1. Pile geometry at Platform BA.

Pile Type	Pile ID	Diameter (mm)	Wall thickness (mm)	Length below mudline (m)
Main pile	A1,	609.6	25.4	91.4
	A2,			
	B1,			
	B2			
Shear pile	S1,	609.6	25.4	39.6
	SA,			
	SB			

3 SOIL PROFILES AT PLATFORM BA

According to soil data at Platform BA location, the soil profile encountered at Platform BA location is characterised by normally consolidated clays, with sand layers found between depth of 38.4-64.6 m and 76.2-83.8 m. Alternating sand and clay layers are reported between 30.8 and 38.4 m; for calculation purposes, this depth interval was assumed as clay material.

For Platform BA location, a ratio $s_u/\sigma'_{v0} = 0.2$ was considered. The ratio of initial stiffness ratio, $G_0/s_u = 350$, anisotropy ratios $s_u^{DSS} / s_u^C = 0.86$ and $s_u^E / s_u^C = 0.75$ were assumed in lack of site-specific information. OCR was assumed as 1.0 throughout the profile, with the exception of the layer at 30.8-38.4 m (alternating clay and sand); here, an OCR = 2.5 was back-calculated based on SHANSEP correlation (Ladd & Foott, 1974).

4 SHALLOW GAS AND EXCESS PORE PRESSURE

At a conceptual level, it is assumed that some of the gas being extracted from the reservoir and travelling along the conductor can escape into the adjacent soil. The extremely small pore size of the clay does not allow the gas to penetrate such material. However, the same gas can propagate within more porous, sandy layers. The presence of gas in these layers has the effect of increasing the otherwise hydrostatic excess pore pressure (XPP). When this XPP transfers to the adjacent clay layers, a reduction in effective stresses, and consequently the s_u is modified. It is important to notice that s_u would constantly re-adjust in time, as a function of the (i) depletion of the reservoir, (ii) level of gas pressure in the gas-charged layers, and (iii) the dissipation of XPP in clay.

The reduction in s_u for clay layers, due to increased XPP can be calculated according to Equation 1 (Ladd & Foott, 1974):

$$s_{u, epp} = \left(\frac{s_u}{\sigma'_{v0}} \right)_{NC} \cdot \sigma'_{v, epp} \cdot OCR^{0.85} \quad (1)$$

Where $(s_u/\sigma'_{v0})_{NC}$ is the normally consolidated strength ratio (0.20 at Platform BA location), $\sigma'_{v, XPP} = (\sigma'_{v0} - XPP)$ is the reduced vertical effective stress due to XPP and OCR is the over-consolidation ratio (assumed as 1.0 at Platform BA location).

In the absence of XPP field measurements at the Platform BA location, a reduction in s_u due to an XPP of 100 kPa in the sand layer is suggested as a guidance for assuming realistic XPP values based on regional experience around Offshore Malaysian Waters. While it is acknowledged that gas might also be present at shallower depths, it is also less likely for it to remain trapped in the soil and cause a disturbance. Hence, only the sand layer below 38.4 m was considered gas-charged in this study.

Above the gas-charged layer, the value of XPP reduces to zero at seabed with an exponential trend. Below the gas-charged layer, the XPP decreases according to the theoretical solution for a distributed load on elastic space (Steinbrenner, 1934).

A graphical illustration of the effect of XPP on σ'_v , and consequently on s_u , is shown in Figure 1 for the Platform BA location (case XPP = 100kPa).

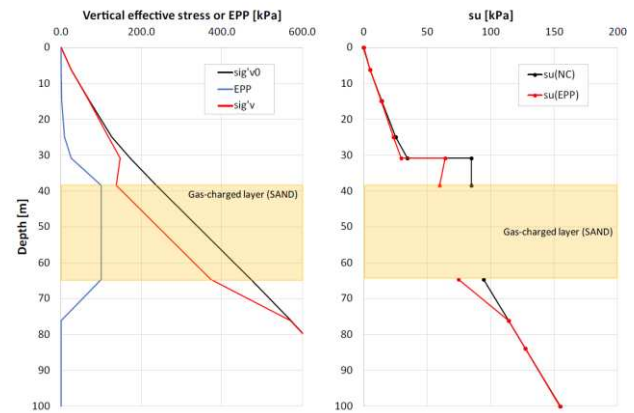


Figure 1. Variation of σ'_v as a function of XPP (LHS) and consequent variation of s_u (RHS) for XPP = 100kPa at Platform BA location

5 METHODOLOGY

5.1 Lateral Response: P-Y curves

P-Y curves can be defined according to different methods proposed in relevant codes and publications. For this work, three P-Y methods were used, namely, API (2014), NGI-PETRONAS (Nichols et al., 2014) and Jeanjean et al. (2017). Whereas API (2014) provides P-Y curves for both clay and sand, the other two methods only offer p-y curves for clay. When analysing sand layers using NGI-PETRONAS

(Nichols et al., 2014) and Jeanjean et al. (2017), API (2014) solution was used.

Each method also distinguishes between for static and cyclic loading conditions. For cyclic conditions under API (2014), the capacity is capped at $0.72 p_u$, where p_u is the ultimate lateral bearing capacity according to Matlock (1970). A degree of softening is applied for depth less than the depth of reduced resistance, Z_R .

For cyclic conditions under NGI-PETRONAS (labelled as “NGI-P” herein) and Jeanjean et al. (labelled as “Jeanjean” herein), the method described in Zhang et al. (2017) was adopted. The method offers a simplified way to scale static p and y as a function of equivalent number of cycles, N_{eq} , along the pile (see Figure 2). Since it was validated with a limited number of Finite Element Analyses (FEA), the method is only valid for a cyclic over average load ratio, $CLR = 1.43$. A constant value, $N_{eq} = 10$ was assumed from regional experience (with N_{eq} increasing linearly from 1 at $p/p_u = 0.0$ to 10 at $p/p_u = 1.0$).

The axial and torsional responses, often analyzed using analogous approaches that implement q - z and t - z curves, were evaluated using the methodology outlined in API (2014).

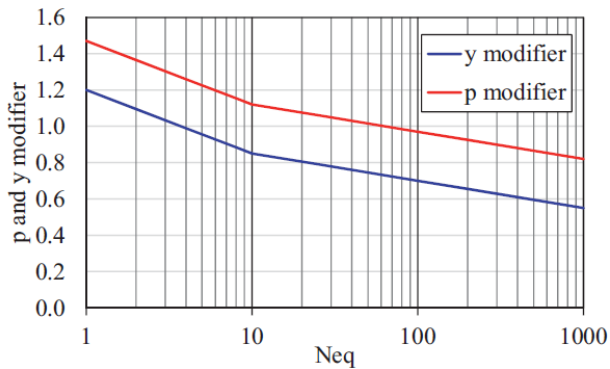


Figure 2. p and y modifiers for different N_{eq} . After Zhang et al. (2017)

5.2 Axial Pile Capacity

For axial pile capacity, the skin friction was calculated using the methods in Table 2:

Table 2. Skin friction computation method

API (2014)	American Petroleum Institute, API (2007) Considers piles both in sand and in clay.
NGI-05 (2005)	Norwegian Geotechnical Institute Piles in clay: Karlsrud et al (2005) Piles in sand: Clausen et al (2005)

For both methods, the tip resistance acting against a closed-ended or plugged pile is calculated as:

$$Q_{tip} = 9 \cdot s_u \cdot A_{tip} \quad (2)$$

where s_u is the undrained shear strength, A_{tip} is the gross pile tip area, $0.25\pi D^2$. The unconfined, undrained shear strength, s_u^{un} is used.

5.3 Effect of Aging on Pile Capacity

It is known from practical experience that pile skin friction increases with time, even after the excess pore water pressures set up during pile driving have dissipated. This increase is observed for piles in both clay and in sand.

After completed consolidation, the skin friction will continue to increase because of ageing effects. Based upon practical experience, it is assumed that the pile skin friction increases linearly with time on a log plot (Skov & Denver, 1988):

$$Q = Q_0 \cdot [1 + \Delta_{10} \cdot \log_{10}(t/t_0)] \quad (3)$$

where $Q(t)$ = Pile skin friction force at time t (kN), $Q(t_0)$ = Pile skin friction force at reference time t_0 (kN), t = Time since pile driving (days), t_0 = Reference time since pile driving (days), Δ_{10} = Dimensionless soil parameter determined from pile field tests.

5.3.1 Determination of Δ_{10}

For piles in clay, the Δ_{10} is calculated using the following equation as per NGI (2013):

$$\Delta_{10} = 0.05 + 1.3 \cdot (1 - I_p / 50)^2 \cdot OCR^{0.5} \quad (4)$$

Where I_p = Plasticity index (%), OCR = Over consolidation ratio

5.3.2 Time needed for re-consolidation for clay layer

The reference time t_0 , which is defined as a time needed for re-consolidation, in Equation 3 is typically taken as 10 days for a sand layer, and 100 days for a clay layer.

The remaining excess pore water pressure at the pile surface after a given time can be estimated from consolidation theory using the below formulae and the diagrams shown on Figures 3 and 4, taken from Karlsrud (2012, 2014).

$$T = t \cdot c_{vh} / r_o^2 \quad (5)$$

$$r_p / r_o = (G_{50} / s_u)^{0.5} \cdot [(r_o^2 - r_i^2) / r_o^2]^{0.5} \quad (6)$$

where T = Dimensionless time factor, t = Time since pile driving, c_{vh} = Coefficient of consolidation for horizontal water flow and reloading, r_o = Pile outside

radius, r_i = Pile inside radius (zero for a pile driven with a closed tip), r_p = Radius of the plastified soil zone near the pile from the pile outside, G_{50} = Clay shear modulus at 50 % strength mobilization, s_u = Undrained shear strength from UU or DSS tests.

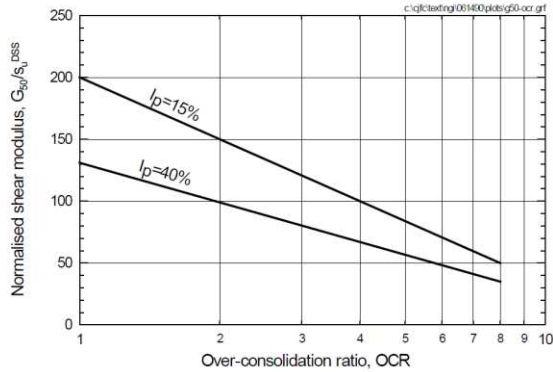


Figure 3. Clay secant shear modulus G_{50} at 50% strength mobilisation, from DSS test on Norwegian clays, from Karlsrud (2012,2014)

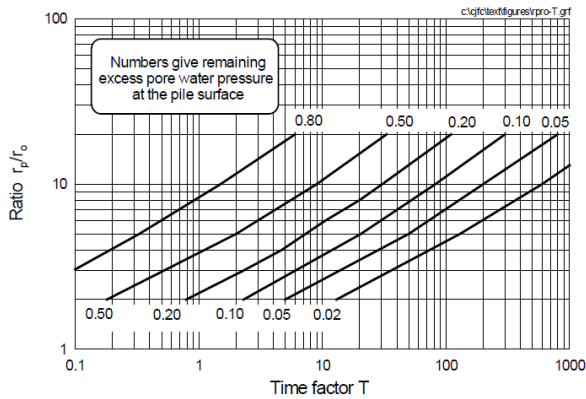


Figure 4. Diagram for determination of remaining excess pore water pressure $\Delta u(t) / \Delta u(t=0)$ at the pile surface, from Karlsrud (2012, 2014)

5.3.3 For piles in sand

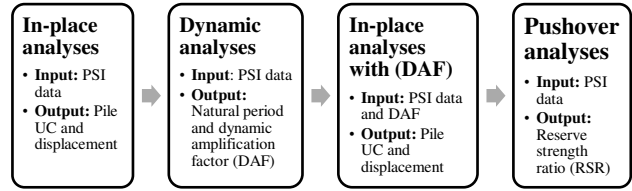
For piles in sand, the majority of the increase in bearing capacity is observed within the first two years. After this period, the effect of aging on bearing capacity becomes negligible (Karlsrud et al., 2014). The test results from piles in Larvik, which have similar soil conditions to the sand layer at Platform BA, are used for estimation. Consequently, the increase in shaft capacity due to aging is estimated to be a factor of 1.7.

5.4 Structural Analyses

Three types of structural analyses were conducted to evaluate the performance of Platform BA. The P-Y, T-Z, and Q-Z data were compiled and utilized as Pile/Soil Interaction (PSI) data for these analyses. The T-Z and Q-Z data were generated according to API (2014). The current state of the Platform BA was initially based on PSI data calculated from API

(2014). Figure 5 below outlines the structural analyses phases with input and outcome from the analyses:

Figure 5. Structural analyses phases

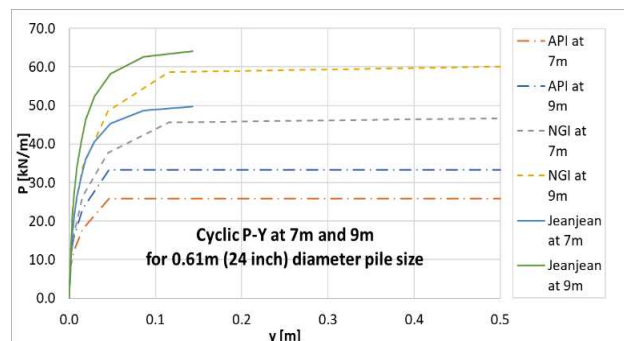


6 RESULTS OF ANALYSES

6.1 Lateral Response (P-Y) curves results

The NGI-P and Jeanjean methods exhibit a stiffer behaviour than the API method. Note that, on the one hand, G_0/s_u is a direct input of the NGI-P method ($G_0/s_u = 350$). On the other hand, Jeanjean provides normalised p-y curves only for $G_0/s_u = 500$ (in lack of DSS tests). Hence, the stiffer curve for Jeanjean compared to NGI-P (the two methods provide seemingly identical curves when the same G_0/s_u is used). Figure 6 show an example of the results at 7m and 9m depths at Platform BA location. The ultimate lateral capacity, p_u , for API method is considerably lower throughout the entire soil profile when compared to NGI-P and Jeanjean.

Finally, a parametric study looked at the effect of a varying XPP level within the sand layer on the pile lateral response. Values of XPP = 0, 50, 100 and 200 kPa were analyzed. The magnitude of XPP within the gas-charged layer did not have any meaningful effect on pile response. Figure 7 shows a summary of lateral displacement, u_y , at pile head for different p-y methods and XPP profiles, Platform BA location. In both cases, it is seen that increasing XPP does not lead to any meaningful increase in u_y . In line with the discussion on p-y curves, the API method consistently produces higher lateral displacements, followed by the NGI-P and Jeanjean methods.



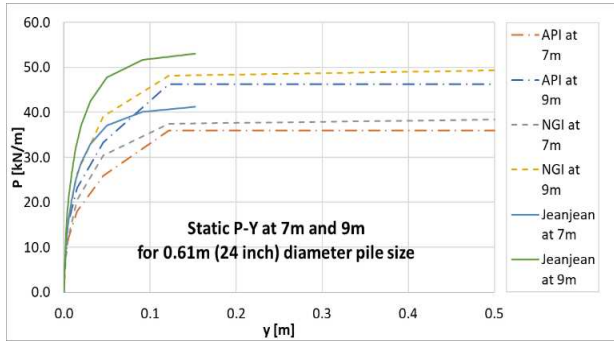


Figure 6. P-Y curves for cyclic and static at 7m and 9m below seabed

The independence of pile lateral response on the level of XPP is because at the locations analysed, the gas-charged layer is very deep (below 38.4 m) with respect to the section of the pile mobilised laterally (roughly top 25m). In other words, the s_u reduction brought about by XPP (Equation 1) in the layers that contribute the most to the lateral response is negligible (see also top 25 m of XPP approaching zero in Figure 1).

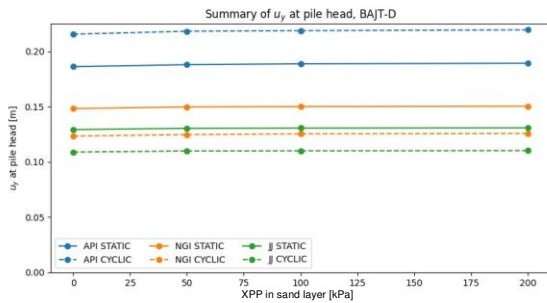


Figure 7. Summary of lateral displacement, u_y , at pile head for different p-y methods and XPP profiles at Platform BA location

6.2 Axial pile capacity results

Based on the modified soil shear strength parameters to account for the effect of XPP (Equation 1), the axial pile capacity for piles A2, B2, and B1 does not meet the required safety factors (SF) for both operating and storm loading conditions using the API and NGI axial pile capacity methods.

The application of the ageing effect to the skin friction resulted in an increase of axial pile capacity from 5.7MN to 9.7MN. This enhancement ensures compliance with the minimum required safety factors of 2.0 for operating conditions and 1.5 for storm conditions. Figure 8 illustrates the axial pile capacity curves before and after the application of the ageing effect. Table 3 provides a summary of the axial pile capacity check for Platform BA.

Table 3. Summary of axial pile capacity check for Platform BA

Pile ID	Total load at pile tip (kN)	Axial pile capacity (no ageing effect) (kN)	Axial pile capacity (with ageing effect) (kN)	Old SF	New SF
Operating Condition					
A1	2548.28	5700	9700	2.24	3.81
A2	3023.49			1.89	3.21
B1	2628.85			2.17	3.69
B2	3089.07			1.85	3.14
Storm Condition					
A1	2918.3	5700	9700	1.95	3.32
A2	2655.4			2.15	3.65
B1	4261.24			1.34	2.28
B2	3513.72			1.62	2.76

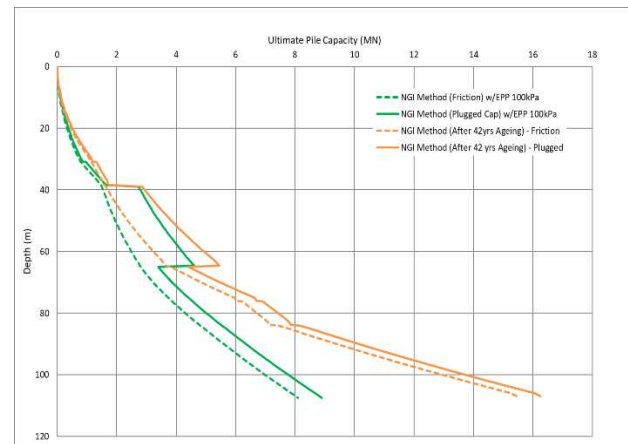


Figure 8. Axial capacity curves before and after ageing effect

6.3 Structural in-place, dynamic and pushover analyses

The structural in-place analysis indicates a positive response to the pile unity check (UC) for both above and below the mudline, corresponding to lateral response as demonstrated by the NGI-P and Jeanjean methods. The maximum lateral deflection at the mudline shows improvement when adopting NGI-P and Jeanjean compared to the API method.

Structural dynamic analyses indicates a minor improvement on the natural period for Platform BA when adopting NGI-P and Jeanjean methods as PSI data. Table 4 shows the summary of structural analyses results based on different lateral response data.

Table 4. Summary of structural in-place and dynamic analyses

Description	Lateral Response (P-Y)		
	API	NGI-P	Jeanjean
Pile UC above mudline	0.681	0.598	0.573

Pile UC below mudline	0.400	0.32	0.280
Max Lateral Deflection at mudline (cm)	6.319	3.265	1.827
Natural Period (sec)	2.304	2.155	2.115

The results from the pushover analyses indicate an improvement when adopting the NGI-P and Jeanjean methods. Notably, enhancements were observed in the directions of 0 and 53.2 degrees, as shown in Table 5.

Table 5. Summary of structural in-place and dynamic analyses

Direction	Reserve Strength Ratio (RSR)		
	API	NGI-P	Jeanjean
0°	3.998	4.221	4.319
53.2°	3.823	3.883	3.898

7 CONCLUSIONS

This study has demonstrated the significant impact of shallow gas on the performance of pile foundations for offshore jacket platforms, specifically Platform BA in Malaysian waters. The presence of gas is linked to the development of XPP in the soil, which affects the effective stresses and ultimately the soil response both axially and laterally.

Understanding the gas phenomena and behavior at the location, such as the possibility that gas at shallower depths might not be trapped, provides a basis for establishing the effect of XPP on soil parameters in lieu of actual monitoring data. This study also highlights the importance of considering the pile ageing effect, which can significantly improve pile axial capacity. The application of the ageing effect to the pile's skin friction resulted in an increase of axial pile capacity from 5.7MN to 9.7MN, ensuring compliance with the minimum required safety factors.

Furthermore, employing newer lateral soil capacity methods, such as the NGI-P and Jeanjean methods, has shown to simulate a stiffer response than the traditional API method, leading to smaller lateral displacement at the pile head. The NGI-P and Jeanjean methods also indicate minimal influence on the pile unity check for piles above and below the mudline, with up to 9% improvement on the offshore jacket platform's natural period and up to 8% improvement on the offshore platform's reserve strength ratio.

Overall, the findings from this study provide valuable insights into the behavior of pile foundations in gas-charged soils and offer practical

solutions for improving the design and performance of offshore jacket platforms.

AUTHOR CONTRIBUTIONS

First Author: Data curation, Formal Analysis, Writing - Original draft. **Other Author:** Software, Conceptualization, Methodology, Supervision. **Additional Authors:** Formal Analysis, Visualization, Investigation. **Last Author:** Writing-Reviewing and Editing.

ACKNOWLEDGEMENTS

The authors are grateful for the support provided by all parties, both from PETRONAS and NGI.

REFERENCES

- American Petroleum Institute (2014). API Recommended Practice 2GEO/ISO 19901-4, Geotechnical and Foundation Design Considerations, 1st Edition, April 2011 Addendum 1.
- Lunne, T., Md. Isa, O., and Tan, M. (1996). Shallow Gas Problem at Duyong B Offshore Malaysia. The 11th Offshore South East Asia Conference. OSEA96065.
- Jeanjean, P., Zhang, Y., Zakeri, A., Andersen, K.H., Gilbert, R., and Senanayake, A.I.M.J. (2017). A framework for monotonic p-y curves in clays. In Offshore Site Investigation Geotechnics 8th International Conference Proceeding (Vol. 108, No. 141, pp. 108-141). Society for Underwater Technology.
- Karlsrud, K. (2012). Prediction of load-displacement behavior and capacity of axially loaded piles in clay based on analyses and interpretation of pile load test results. Thesis for the degree of Doctor Philosophiae. Norwegian University of Science and Technology. ISBN 978-82-471-3471-9. ISSN 1503-8181.
- Karlsrud K., Jensen T.G., Lied E.K.W., Nowacki F., and Simonsen A.S. (2014). Significant Ageing Effects for Axially Loaded Piles in Sand and Clay Verified by New Field Load Tests. OTC-25197-MS.
- Ladd, C.C., and Foott, R. (1974). New design procedure for stability of soft clays. Journal of the geotechnical engineering division, 100(7), 763-786.
- Matlock, H. (1970), Correlations for Design of Laterally Loaded Piles in Soft Clay. Proc. 2nd

- Annual Offshore Technology Conference (OTC), Houston, Texas, April, 1970. OTC-1204.
- Skov, R. and Denver, H. (1988). "Time- dependence of bearing capacity of piles". Proc. 3rd Int. Conf. on the application of stress-wave theory to piles. Ottawa, Canada, pp. 879-888.
- Long, M. & Donohue, S. (2010). Characterization of Norwegian marine clays with combined shear wave velocity and piezocone cone penetration test CPTU data. Canadian Geotechnical Journal, 47(7), pp. 709-718.
- Nichols, N.W., Rohani M.J., Mukherjee, K., Ayob, M.S., Clausen, C.J., and Lunne, T. (2014). Effect of lateral soil strength and stiffness on jacket foundation integrity and design for South China Sea sites. OTC-24842-MS.
- Steinbrenner, W. (1934). Tafeln zur setzungsberechnung. Die StraBe, 1.
- Rohani, M.J., Azam, A.R., Strout, J.M., and Lunne, T., (2014). Foundation Integrity: Shallow Gas Mitigation Using the XPP Monitoring Tool – An Offshore Malaysia Case History. OTC-24843-MS.

INTERNATIONAL SOCIETY FOR SOIL MECHANICS AND GEOTECHNICAL ENGINEERING



This paper was downloaded from the Online Library of the International Society for Soil Mechanics and Geotechnical Engineering (ISSMGE). The library is available here:

<https://www.issmge.org/publications/online-library>

This is an open-access database that archives thousands of papers published under the Auspices of the ISSMGE and maintained by the Innovation and Development Committee of ISSMGE.

The paper was published in the proceedings of the 5th International Symposium on Frontiers in Offshore Geotechnics (ISFOG2025) and was edited by Christelle Abadie, Zheng Li, Matthieu Blanc and Luc Thorel. The conference was held from June 9th to June 13th 2025 in Nantes, France.